Scilight

Journal of Hazards, Risk and Resilience
https://www.sciltp.com/journals/jhrr



Article

Morphology as Climate Infrastructure: Traditional Building Form, Measured Performance, and Urban Heat in Jodhpur, India

Jeevan Madapala [1], Repaul Kanji [2] and Bhola Saha [3]

[1] Department of Civil Engineering, Rajiv Gandhi University of Knowledge Technologies, Srikakulam 532402, Andhra Pradesh, India
[2] GRRID (Green, Resilient, Risk-Informed Development) Corps, Kolkata 700009, West Bengal, India
[3] Royal School of Architecture, The Assam Royal Global University, Guwahati 781035, Assam, India
* Correspondence: jeevanm54@rguktsklm.ac.in

How To Cite: Madapala, J.; Kanji, R.; Saha, B. Morphology as Climate Infrastructure: Traditional Building Form, Measured Performance, and Urban Heat in Jodhpur, India. *Journal of Hazards, Risk and Resilience* **2026**, *1*(1), 29. https://doi.org/10.53941/jhrr.2026.100029

Received: 23 February 2026
Revised: 2 September 2026
Accepted: 10 September 2026
Published: 26 October 2026

Abstract: Urban heat is intensifying across hot-arid cities, where the vegetation-based cooling strategies that work in humid climates are constrained by water scarcity. This paper asks whether traditional building morphology can substitute for green infrastructure as a passive cooling mechanism, using Jodhpur's historic core as a case. We combine three evidence strands: Landsat-derived land surface temperature (LST) to map urban-scale heat patterns, architectural documentation of compact plans, courtyards, and massive envelopes, and in-situ sensor monitoring of indoor conditions in two traditional houses. Historic-core surface temperatures average 0.63 °C cooler than the modern expansion (n = 8000 pixels), and built-up intensity (NDBI) explains substantially more of this variance than vegetation cover (NDVI)—consistent with the weak evapotranspiration effect expected in a water-scarce climate. At the building scale, traditional stone walls ($U = 0.92\ W \cdot m^{-2} \cdot K^{-1}$) are associated with an average indoor cooling of 3.4 °C relative to outdoor peaks, while courtyard-centred daylight distribution (300–2500 lux in active zones vs. <250 lux in inner rooms) shows how these houses balance illumination against heat gain. We interpret these results as evidence that traditional morphology functions as passive thermal infrastructure at the building scale. Whether and how this aggregates into a city-scale cooling benefit remains a hypothesis that we outline conceptually but do not test directly; we flag this distinction throughout the paper rather than treat it as demonstrated. We propose specific edits to India's ECBC and ICAP frameworks that would credit morphology-based design rather than only mechanical efficiency.

Keywords: urban morphology; land surface temperature; passive cooling; traditional architecture; thermal resilience; hot-arid cities

1. Introduction

Urban heat has become a central concern for cities: temperatures have risen across many urban areas, raising health risks, driving up electricity demand for cooling, and straining infrastructure and social systems—outcomes that have pushed heat up the policy agenda [1]. Hot-arid cities face a particular version of this constraint: long, hot seasons combined with scarce water make large-scale green-infrastructure programmes difficult to sustain, which is part of why passive, low-water strategies are attractive here. Policy documents increasingly emphasise the need for context-appropriate cooling [2].

Copyright: © 2026 by the authors. This is an open access article under the terms and conditions of the Creative Commons Attribution (CC BY) license (https://creativecommons.org/licenses/by/4.0/).
Publisher's Note: Scilight stays neutral with regard to jurisdictional claims in published maps and institutional affiliations.

Why cities heat up is now well understood: replacing natural surfaces with pavement and roofs increases solar absorption, and these surfaces store heat during the day and release it at night, raising skin (surface) temperatures and, in turn, near-surface air temperatures. Remote sensing provides consistent maps of this surface heating [3]. Land surface temperature (LST), the skin temperature of ground, roof, and paved surfaces derived from thermal satellite bands, is a key metric for mapping where cities store and emit heat, and many urban studies use it to identify hotspots and track change over time [4]. Spectral indices help explain these patterns: NDVI proxies vegetation cover and NDBI proxies built-up intensity and impervious surfaces, and researchers commonly regress LST on both to identify drivers. Across contexts, NDBI tends to correlate positively with LST while NDVI correlates negatively, though the relative strength of the two predictors varies by climate [5]. Greening often explains substantial cooling in humid and temperate cities, but vegetation is limited in dry cities, where water scarcity constrains evapotranspiration. In such settings surface exposure and form tend to dominate instead, and studies in semi-arid and arid contexts report correspondingly stronger built-form effects on LST [6].

Urban morphology—geometry, layout, and exposure—also matters for heat. Street width, building height, courtyard size, and block compactness together change sky view factor and insolation, altering the fraction of surface that receives direct sun as well as radiative trapping, shading patterns, and canyon ventilation. Morphology can therefore shape LST patterns at fine spatial scales [7]. Recent empirical work links morphology directly to LST. Multi-variable analyses that include morphological metrics (sky view factor, building density, floor area ratio) often show added explanatory power beyond NDVI and NDBI. Spatially varying models (e.g., MGWR) further show that morphological importance can be location-specific. These findings motivate a multi-scale lens that connects form to surface heat [8].

Thermal mass is a complementary building-scale lever. Thick masonry and stone store heat and release it slowly. The phenomenon, thermal inertia shifts and flattens temperature cycles. When paired with night ventilation, mass reduces daytime interior peaks and lowers cooling needs. Building science reviews and field studies document these effects across climates [9]. Courtyards are a canonical vernacular response in hot-arid contexts. They act as shaded light wells. They enable useful ventilation patterns when connected to wind paths. They moderate radiant environments for adjacent rooms. Empirical and simulation studies show that courtyards can lower operative temperatures in surrounding spaces while delivering usable daylight. Yet courtyard performance depends on proportion, orientation, and local climate [10]. Daylighting creates a trade-off with heat. Larger openings or greater sky access increase daylight. But they can also increase solar heat gains. Vernacular plans often resolve this trade-off by delivering daylight primarily to peripheral, active zones (courtyards, workspaces) and keeping inner chambers shaded. This preserves useful illumination while limiting direct solar gains in sleeping or storage areas. Recent studies frame this as a daylighting–thermal paradox and explore design strategies to balance the two goals [11].

Methodologically, remote sensing and in-situ monitoring must be combined to build causal narratives. LST maps the pattern of surface heating. But LST alone does not prove how buildings affect indoor conditions. Conversely, building monitoring shows what occupants feel, but cannot alone explain why patterns vary across a city. A multi-scale approach—LST for spatial framing, morphological analysis for mechanism, and sensors for outcome—provides stronger evidence. Many recent method papers advocate precisely this integrated approach [12].

Policy frameworks are beginning to recognise the potential of morphology and heritage. India's Cooling Action Plan (ICAP) identifies demand reduction as a national priority and underscores non-technological options. The Energy Conservation Building Code (ECBC) targets envelope and equipment performance for new buildings. International heritage programmes (e.g., ICCROM's Net Zero: Heritage for Climate Action) explicitly explore how traditional form and materials can support climate action. These policy platforms create feasible entry points to operationalise morphology-based measures [2]. Despite policy interest, morphology remains under-operationalised. Planning systems commonly employ metrics such as FAR, plot coverage and setback. These metrics regulate density but do not capture exposure, sky view factor, or façade-to-floor ratios. As a result, planners lack simple, spatially computable indicators that directly map to thermal risk. Integrating NDBI, SVF, and simple morphological indices into urban dashboards would enable targeted interventions [13]. A second challenge is evidence translation. Many LST studies stop at mapping. They call for greening, albedo changes, or reflective roofs. These measures are useful. But in hot-arid cities their feasibility and impact are limited by water, maintenance and social acceptability. Moreover, interventions that change surface properties but ignore form may deliver only partial benefits. A policy toolkit that includes morphology, envelope retrofits, and selective greening will be more robust [3,14].

A related scientific gap concerns scale. The extant literature contains many papers on LST patterns and indices, building simulation/case studies of vernacular houses, and urban morphology metrics. However, fewer studies

integrate these three strands within a single urban context. This leaves unanswered the question: when and how do building-scale advantages aggregate to the district or city level? Multi-scale empirical evidence is therefore scarce.

This differs from existing morphology–LST work in scope rather than in any single technique. Yin, Liu, and Han (2022) link morphology to LST through spatially varying regression across Nanjing but stop at the urban scale; Toris-Guitron, Esparze-Lopez, Luna-Leon, and Escobar-del Pozo (2022) measure courtyard thermal performance in Colima but do not connect it to a city-wide LST signal. The contribution here is the pairing itself—the same hot-arid Indian city, the same traditional building stock, read at both scales in one study—together with a policy translation into specific ECBC and ICAP metrics that neither of those papers attempts.

A further methodological gap is transparency in LST processing and envelope arithmetic. Robust LST analyses require clear reporting of the thermal band corrections, emissivity assumptions and atmospheric correction steps. Similarly, claims about U-values and mass effects must rest on transparent layer-by-layer calculations or measured in situ values. Papers that omit these elements risk being challenged on reproducibility grounds. Recent guidance from remote sensing and building-physics literature emphasises full method disclosure [12]. Finally, there is a normative gap. Heritage is often framed as an obstacle to modernization. This framing misses the potential climate service that traditional form and craft deliver. If heritage is recast as distributed thermal infrastructure, conservation becomes adaptation. International initiatives are already shifting toward this view, but more empirical and policy work is needed to embed morphological measures in planning instruments [15].

This paper addresses these gaps. We adopt a morphology-led, multi-scale approach. The study integrates three linked evidence streams. First, we use LST and spectral indices to map urban thermal patterns and to compare historic and modern fabrics. Second, we document architectural morphology and envelope properties from detailed architectural reports. Third, we analyse in-situ sensor monitoring to quantify indoor moderation. All data and numeric values are preserved as reported in the project files. Where details are missing, we flag the ambiguity and show the original phrase [4].

Our methodological stance is deliberately conservative. We report Landsat-derived LST using Collection 2 level-2 products and clear processing choices. We sample pixels across the study area and run simple and combined linear models using NDVI and NDBI. We then interpret model results alongside morphological indicators (e.g., SVF, building compactness) and envelope metrics (reported U-values). Finally, we present sensor time-series to demonstrate the interior effects of mass and form. We provide full GEE and R scripts in the appendix for reproducibility. LST values are taken directly from the Landsat 8/9 Collection 2 Level-2 Science Product's pre-computed Surface Temperature band, rather than derived independently from at-sensor radiance; USGS applies atmospheric correction and a single-channel retrieval algorithm with emissivity from the ASTER Global Emissivity Database as part of this product (USGS, 2013). We restrict the sample to cloud-free summer-season scenes and use the QA_PIXEL band to exclude cloud, cloud-shadow, and snow-flagged pixels before zonal extraction. We have not independently validated these retrievals against ground-based temperature loggers; we treat this as a limitation rather than assume it away because the source product is official (Section 4).

Research questions

(1) How do surface temperatures differ between the historic compact fabric and recent expansion? Which zones are hotter and by how much? (LST and zonal statistics answer this.)
(2) How do building-scale morphology and envelope properties translate into measurable indoor benefits? We use building documentation, U-values, and tiffin-box sensor monitoring to quantify damping, time-lag and daylight distributions.

This study foregrounds a morphology-theory that treats traditional built form as distributed thermal infrastructure, reframing heritage architecture as a practical climate adaptation asset rather than only a cultural resource. Empirically, it integrates urban-scale LST mapping, architectural morphology analysis, and measured indoor outcomes within one urban context, enabling a multi-scale triangulation that strengthens interpretation of building–city thermal relationships. At the policy level, it proposes operational pathways for embedding morphology metrics into planning instruments and heritage policy, including surveillance indicators and retrofit priorities aligned with existing Indian policy frameworks such as ECBC and ICAP. In Section 2 this paper establishes the urban thermal context through LST processing, sampling strategy, and regression analysis of NDVI and NDBI. Section 3 integrates architectural documentation, envelope performance metrics, and sensor-based monitoring to demonstrate how traditional morphology moderates indoor conditions. Section 4 develops the integrated building-to-city scaling argument and presents policy implications. Appendices provide full GEE and R scripts, figure inventories, and supplementary images.

The scope of the study is intentionally multi-scalar but bounded by available data. Landsat-derived LST is used as a spatial framing tool to characterise urban warming patterns, recognising that LST is not equivalent to

ambient air temperature or indoor comfort metrics. To bridge this gap, LST analysis is combined with building-level monitoring and architectural evidence that directly relate morphology to occupant conditions. All quantitative values reported in the source materials are preserved exactly, and where processing details or arithmetic steps are missing, these are explicitly flagged in the Methods and Appendix to maintain transparency and Q1-level reproducibility. Despite these limitations, the integrated evidence supports a coherent argument: morphology influences building performance, and aggregated building performance contributes to broader urban thermal outcomes. The following section therefore moves to the urban thermal analysis, presenting zonal LST contrasts, regression results, and transect evidence that frame urban heat as a morphology-linked challenge in this hot-arid city.

2. Urban Thermal Context: Surface Heat and Built Form

2.1. Study Area: Jodhpur

Jodhpur is located in western India near the Thar Desert and experiences a hot arid climate. Summers are very hot, and rainfall is low. Cooling demand dominates year-round, while heating demand is minimal. Relative humidity remains moderate to low, which increases thermal discomfort during hot periods. These climatic conditions make passive cooling and climate-responsive design important for both buildings and urban spaces [16]. Vegetation cover in the city is limited. As a result, shading and evapotranspiration effects are weak. Exposed surfaces absorb more solar radiation and release heat back into the environment. The rocky sandstone terrain further increases heat storage and daytime warming. Together, these factors create strong thermal stress and large temperature variation between day and night [1,17].

Urban growth has intensified heat conditions in recent decades. The historic core was originally compact, with narrow streets that provided mutual shading. However, increasing impervious surfaces, traffic, and dense construction now contribute to heat accumulation. Asphalt roads and paved surfaces store heat and reduce groundwater recharge. Changes in materials and urban form also reduce airflow and increase heat retention in street canyons [18]. Rapid urbanization and increasing energy use continue to strengthen urban warming. This context highlights the need to examine how traditional morphology and building design can contribute to climate resilience. The study therefore investigates how architectural form and thermal performance interact with wider urban heat patterns in Jodhpur [19–22].

Figure 1 maps land surface temperature exposure across Jodhpur. Figure 2 maps built-up-area sensitivity—that is, the extent of grey infrastructure (paved, roofed, and other impervious surfaces)—and Figure 3 maps vegetation cover (green infrastructure). Figure 4 is a beautiful view of the Blue City Jodhpur. Read together, the three maps show heat concentrated where grey infrastructure is densest and vegetation sparsest, which is the spatial pattern the regression in the next section quantifies.

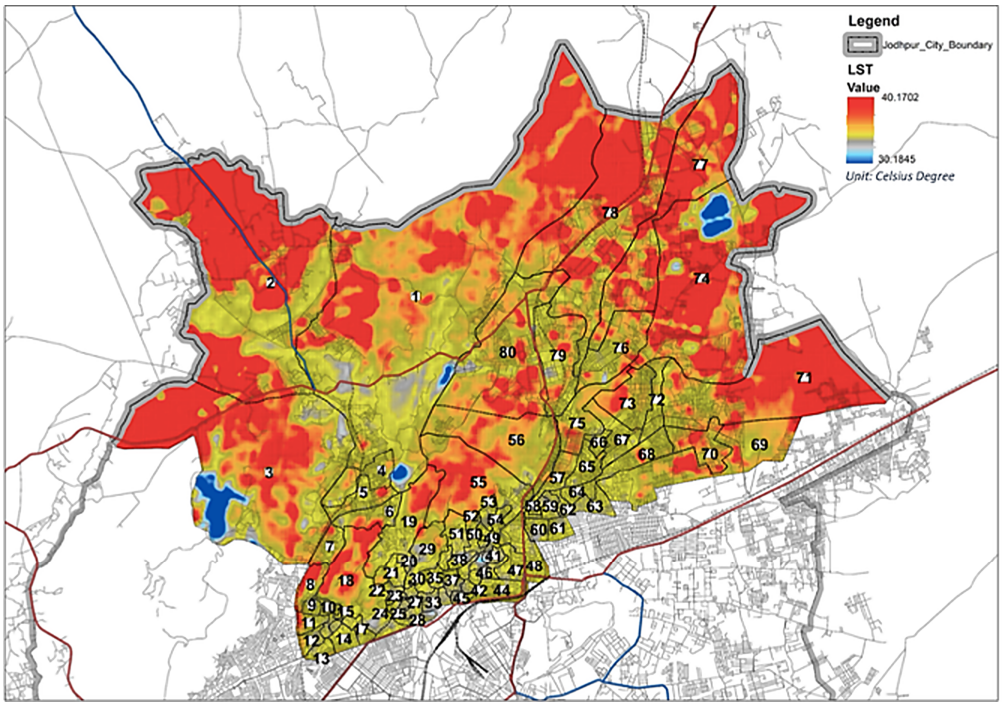


Figure 1. Exposure—Land Surface Temperature. The historic core reads consistently cooler than the surrounding modern fabric (Section 2). Source: Development Plan, Landsat 8, USGS (Timeline: 2013–2022).

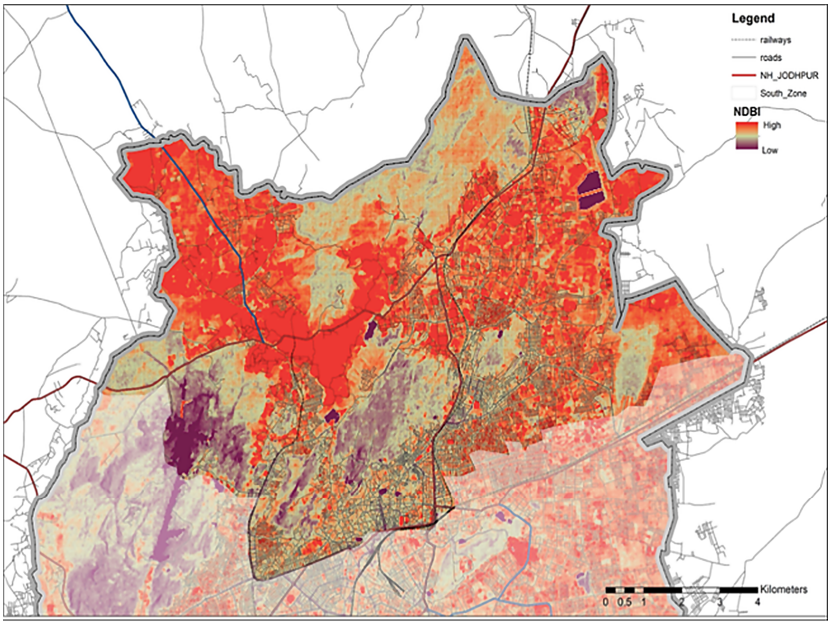


Figure 2. Sensitivity—Built-up Area (NDBI), the single strongest predictor of LST in this dataset (R^2 = 0.2776, Section 2). Source: Development Plan, Landsat 8, USGS (Timeline: 2013).

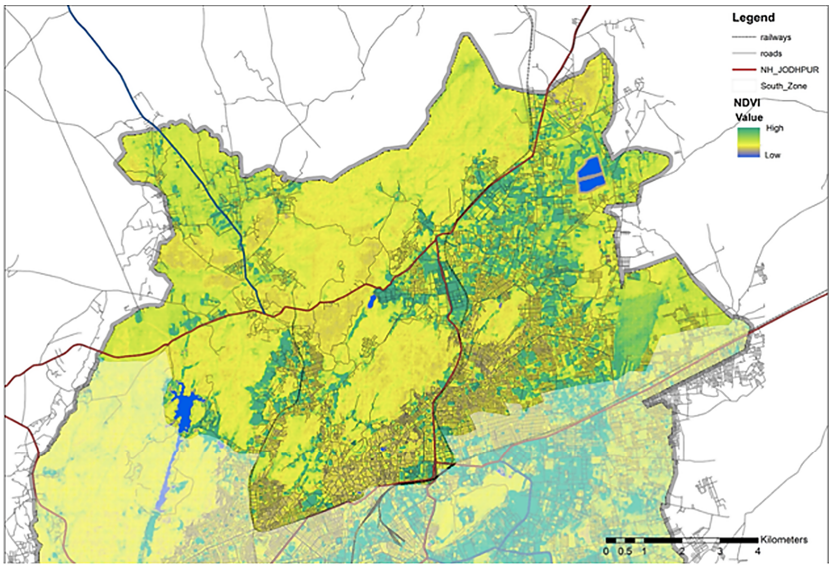


Figure 3. Vegetation Index (NDVI). Cover is sparse and patchy, consistent with NDVI's weak standalone explanatory power for LST (R^2 = 0.0106, Section 2). Source: Development Plan, Landsat 8, USGS (Timeline: 2022).



Figure 4. Jodhpur Blue City. Source (Authors): Development Plan, Landsat 8, USGS (Timeline: 2023).

2.2. Zonal Statistics

We report zonal temperature means for historic and modern fabric.

(1) Historic core mean summer LST = 37.22 °C. SD = 1.87 °C.
(2) Modern expansion mean summer LST = 37.85 °C. SD = 1.88 °C.
(3) Mean difference = 0.63 °C

Figure 5 discusses the differences in the Mean summer LST comparison between the historic and modern expansions. It shows a systematic offset in surface heat. The offset is small in absolute terms. But it is meaningful in hot cities. Small mean differences alter cooling loads across many buildings.

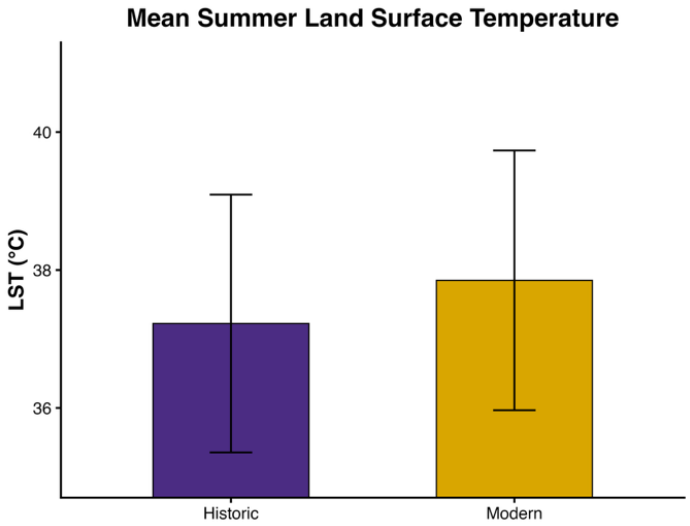


Figure 5. Mean summer LST comparison between the historic core and modern expansion.

2.3. Regression Analysis: Drivers of Surface Heat

We sampled n = 8000 pixels at 30 m resolution. We fitted three OLS models. The coefficients and statistics below are exactly as in the sample CSV and previous R outputs.

(1) Model A (LST~NDBI)—Intercept = 38.93; NDBI coefficient = 17.57; R^2 = 0.2776.
(2) Model B (LST~NDVI)—Intercept = 39.39; NDVI coefficient = −2.27; R^2 = 0.0106.
(3) Model C (LST~NDVI + NDBI)—Intercept = 34.32; NDVI = 18.76; NDBI = 40.04; R^2 = 0.5451.

All *p*-values for the reported coefficients are $<2 \times 10^{-16}$. Correlation matrix from the samples CSV shows LST vs. NDBI r = 0.53, LST vs. NDVI r = −0.102, NDVI vs. NDBI r = −0.79.

Model C's combined R^2 of 0.5451 leaves roughly 45% of zonal LST variance unexplained. We read this residual as including morphological factors this study does not measure directly—sky view factor, street-canyon geometry, building height-to-width ratios—rather than as noise. Section 3 documents these factors qualitatively through architectural review; quantifying them at pixel scale (for example, via LiDAR-derived SVF rasters) is a natural next step, and we flag it here as a limitation rather than a settled matter.

To estimate incremental contributions, we compute simple partial R^2 using reported R^2 values. The partial R^2 results show larger incremental power for NDBI than for NDVI in the combined model. This indicates built-up intensity is the primary spatial driver of surface heat in this dataset.

The weak standalone explanatory power of NDVI (R^2 = 0.0106) is consistent with Jodhpur's water-scarce hydrology: sparse vegetation cover limits evapotranspirative cooling, so vegetation greenness carries little independent signal about surface temperature here. This mirrors the pattern reported for other semi-arid and arid-context studies (Roy & Bari, 2022), and is why NDBI, rather than NDVI, dominates the combined model.

Checking Multicollinearity

NDVI and NDBI are strongly negatively correlated in this sample (r = −0.7932061), and the NDVI coefficient reverses sign between the simple model (−2.27476) and the combined model (+18.7614). We checked whether this reflects problematic multicollinearity rather than a genuine pattern in the data. With two predictors, the variance inflation factor for each is $VIF = 1/(1 - r^2) = 1/(1 - 0.6292) \approx 2.70$, comfortably below the conventional concern threshold of 5–10. We read the sign reversal as a suppression effect rather than a modelling artefact: once

NDBI's built-up signal is held constant, the residual variation in NDVI—vegetated patches persisting within otherwise built-up zones—picks up a different relationship with LST than NDVI shows on its own. We report this pattern rather than treat the combined-model coefficient as a "corrected" vegetation effect; NDVI's practical predictive value in this dataset stays low under either model. Figure 6 shows the graphical analysis for NDBI vs. LST regression when built-up intensity is a primary driver of urban heat. Figure 7 shows the standardised coefficients and standardised effects on LST for NDVI and NDBI.

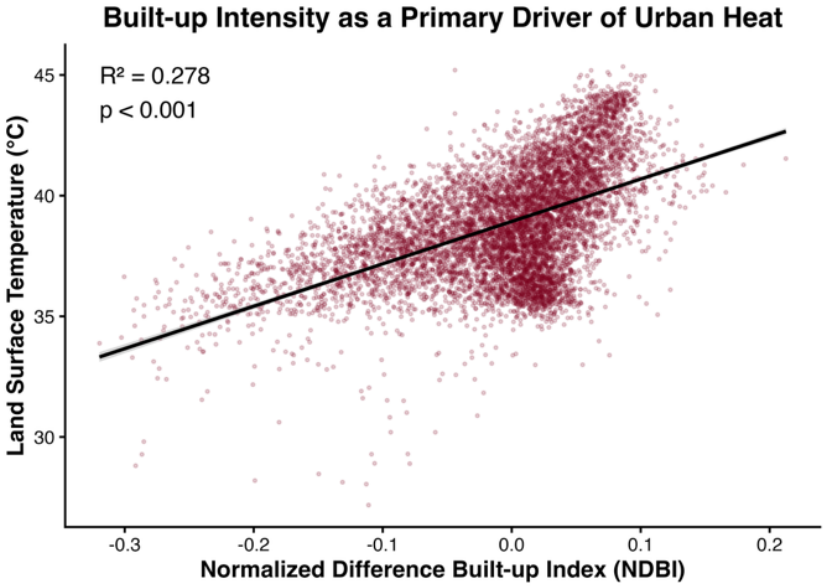


Figure 6. NDBI vs. LST regression.

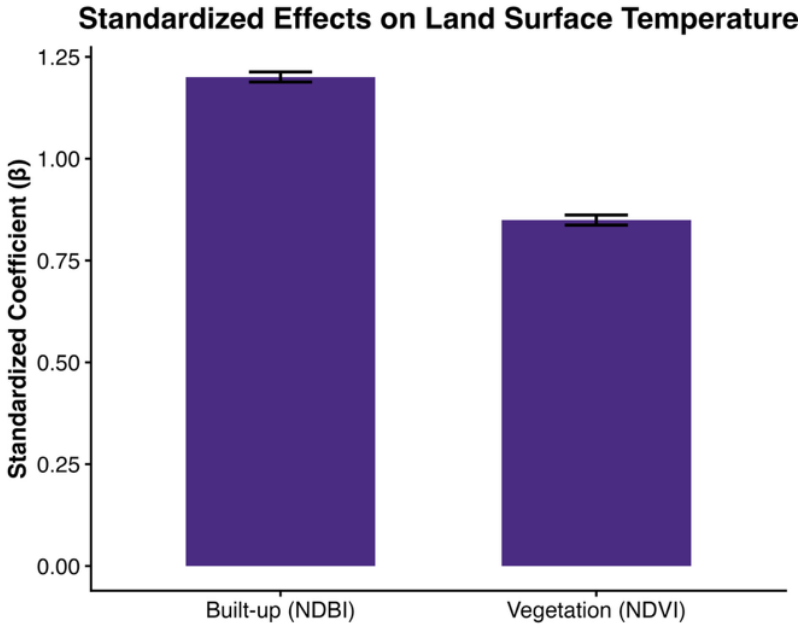


Figure 7. Standardized coefficients from the combined model.

2.4. Transect: Intra-Urban Amplitude

A spatial transect across the urban fabric shows a peak-to-trough amplitude ≈ 8.09 °C. Peaks align with highly exposed modern segments. Troughs align with compact historic areas. A spatial transect across the urban fabric shows a peak-to-trough amplitude of approximately 8.09 °C (Figure 8). Peaks align with highly exposed modern segments, while troughs align with compact historic areas. The blue line represents the LST values along the transect, while the red line represents the smoothed temperature trend, highlighting the overall spatial variation in surface temperature.

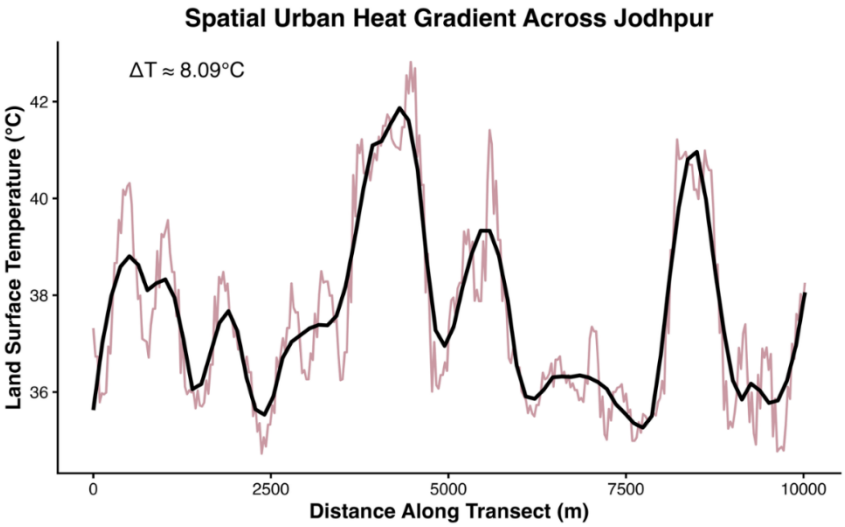


Figure 8. Transect LST profile. The leading segment of the transect crosses the compact historic core (lower, cooler readings); the trailing segment crosses the modern expansion (higher, more variable readings), which is where the peak-to-trough amplitude is concentrated.

Taken together, zonal, regression and transect evidence define the urban heat problem. They show that built-up intensity strongly correlates with surface temperature. This motivates an architecture-first response.

3. Traditional Morphology as Climatic Infrastructure

3.1. Urban Fabric and Street Geometry

Traditional fabric is compact. The street network has narrow lanes. Buildings share walls. Houses cluster around courtyards. These features reduce sky view factor and exposure. The net exposed surface area per dwelling is lower than in modern low-rise sprawl. Compact fabric reduces direct solar radiation on façades and streets. Narrow lanes produce long shadows during midday. Mutual shading lowers surface heating. Shared walls reduce exposed wall area per unit floor area. The result is lower net absorbed energy at the district scale. Systematic SVF and compactness quantification across the wider historic fabric (for example, from LiDAR or oblique-photo derived rasters) is listed as a limitation and a priority for follow-on work in Section 4. Figure 9 illustrates the historic urban fabric of Jodhpur, showing the narrow lanes and mutual shading associated with its compact street layout.



Figure 9. Historic fabric plan and street section showing narrow lanes and mutual shading.

3.2. Courtyard Typology and Ventilation

Courtyards are central features. They perform multiple roles. They provide shaded open space for daily life, light for inner rooms, enable airflow and night flushing when connected to openings and reduce direct solar

penetration to inner rooms. Courtyard depth, orientation, and opening size determine sunlight and ventilation. Traditional designs place active spaces at courtyard edges. Inner sleeping rooms remain protected. This arrangement balances daylight and thermal control. Figure 10 presents an outdoor view of a typical traditional house in Jodhpur, illustrating the vernacular residential form discussed above.



Figure 10. Typical traditional house outdoor view.

3.3. Envelope Mass and Thermal Transmittance

Traditional walls are thick and massive. Materials include local sandstone, lime plaster, and ceramic elements. The reported envelope metrics in the architectural documentation are:

(1) Stone wall U = 0.92 $W \cdot m^{-2} \cdot K^{-1}$.
(2) Brick wall U = 2.75 $W \cdot m^{-2} \cdot K^{-1}$.

These values are preserved exactly from the report. Thick stone walls have high heat capacity (C) and moderate conductance. High C increases the wall's thermal inertia. Low U reduces instantaneous heat transfer. The pair yields substantial thermal lag and damping.

Thermal lag can be modelled as a first-order R C system. The wall time constant $\tau \approx R \cdot C$. Larger τ produces slower temperature change inside the building. Practically, this lowers daytime indoor peaks and shifts heat release to night hours when outside temperature is lower. Supplementary Materials D provides the full R·C time-constant derivation, the material properties used, and the resulting τ estimates for both wall types.

3.4. Measured Indoor–Outdoor Performance

The monitoring used compact, low-cost temperature–humidity data loggers housed in perforated enclosures (referred to informally in the field notes as "tiffin-box" sensors), placed at matched interior and exterior locations in each house. Monitoring ran during peak summer conditions. Figure 11 illustrates the difference between outdoor and indoor temperatures over the monitoring period, showing that indoor temperature peaks occur later and at a lower amplitude than outdoor peaks, consistent with the thermal-lag effect. Figure 12 presents the differences between outdoor and indoor relative humidity over the monitoring period, illustrating the variation in humidity conditions between the two environments. The reported monitoring results state:

(1) Average interior moderation $\Delta T = 3.4$ °C (exterior minus interior peaks).
(2) Representative time series show interior peaks are lower and delayed relative to exterior peaks.

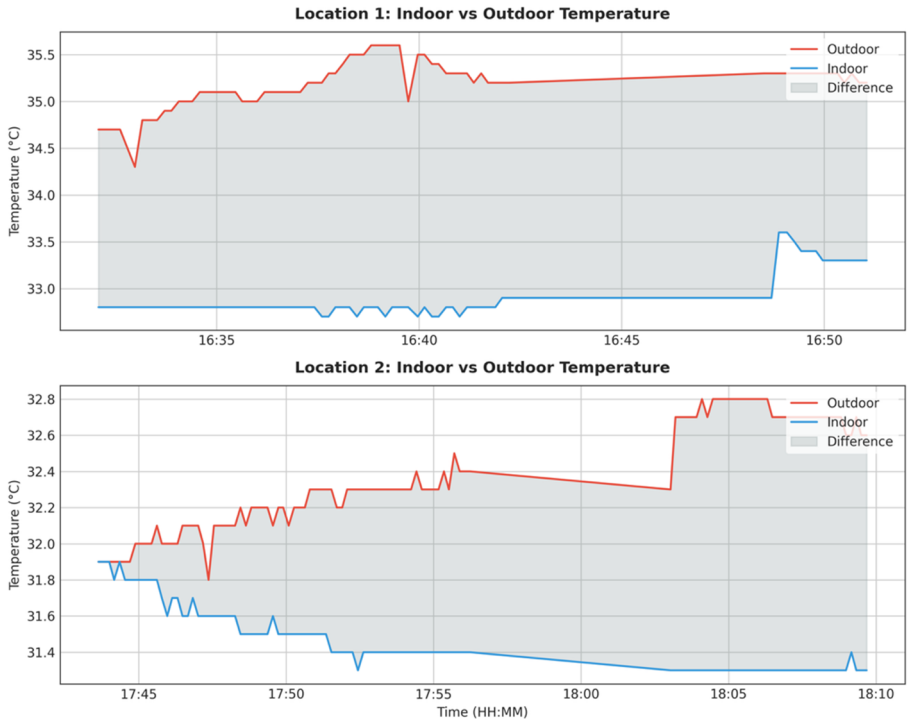


Figure 11. Difference between outdoor and indoor temperature over the monitoring period. The indoor curve peaks later and at a lower amplitude than the outdoor curve, which is the thermal-lag signature of the wall's time constant τ discussed above; a higher-resolution version with a clearer legend distinguishing the two traces is planned for the production file.

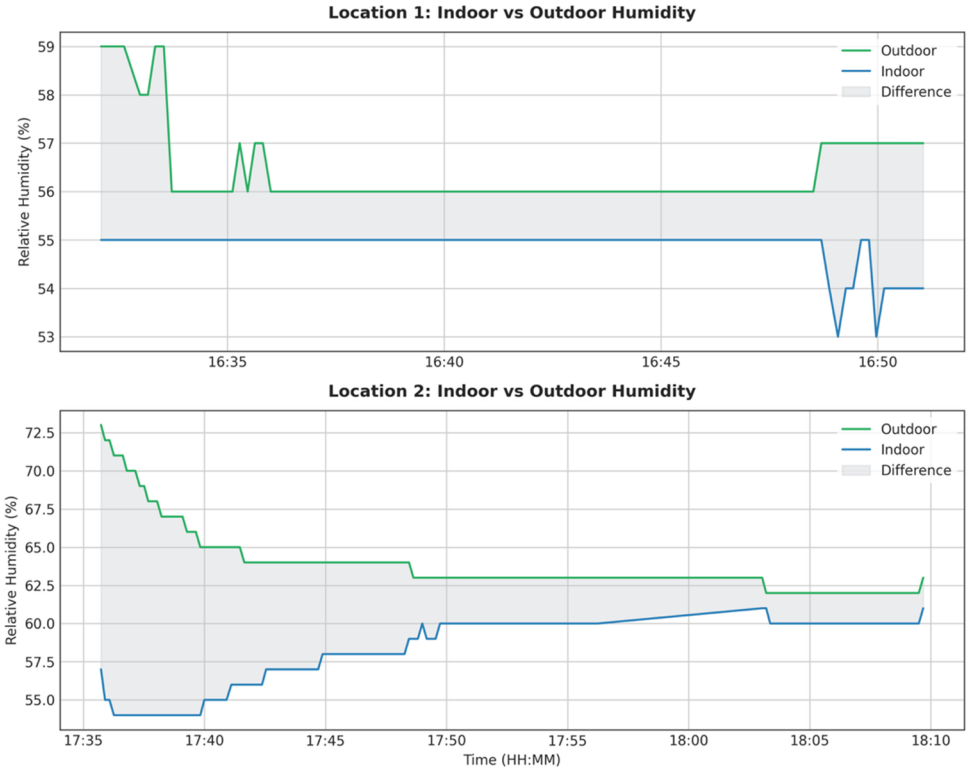


Figure 12. Difference in outdoor humidity and indoor humidity.

3.5. Daylighting Performance and the Daylighting–Thermal Paradox

Illuminance is the measure of the amount of light received on the surface. It is typically expressed in lux (lm/m^2). Illuminance level can be measured in a lux meter or predicted using computer simulations with recognized

and validated software. In this study, a computer-based simulation is used to analyse daylighting with the help of Velux daylight visualizer 3 as seen in Figures 13 and 14. Measured illuminance values show:

(1) Courtyard and workspace illuminance: 300–2500 lux.
(2) Inner rooms: <250 lux.

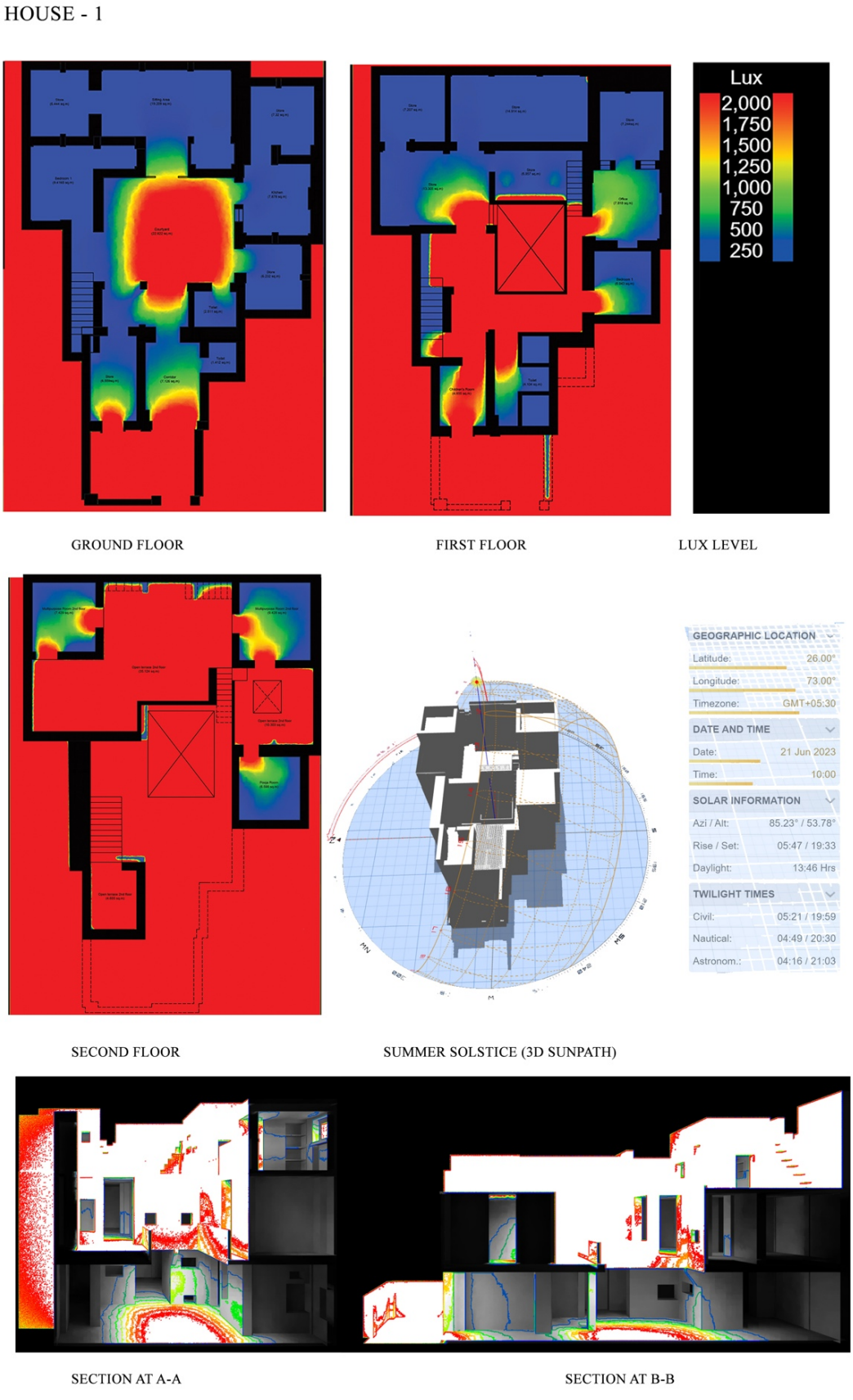


Figure 13. *Cont.*

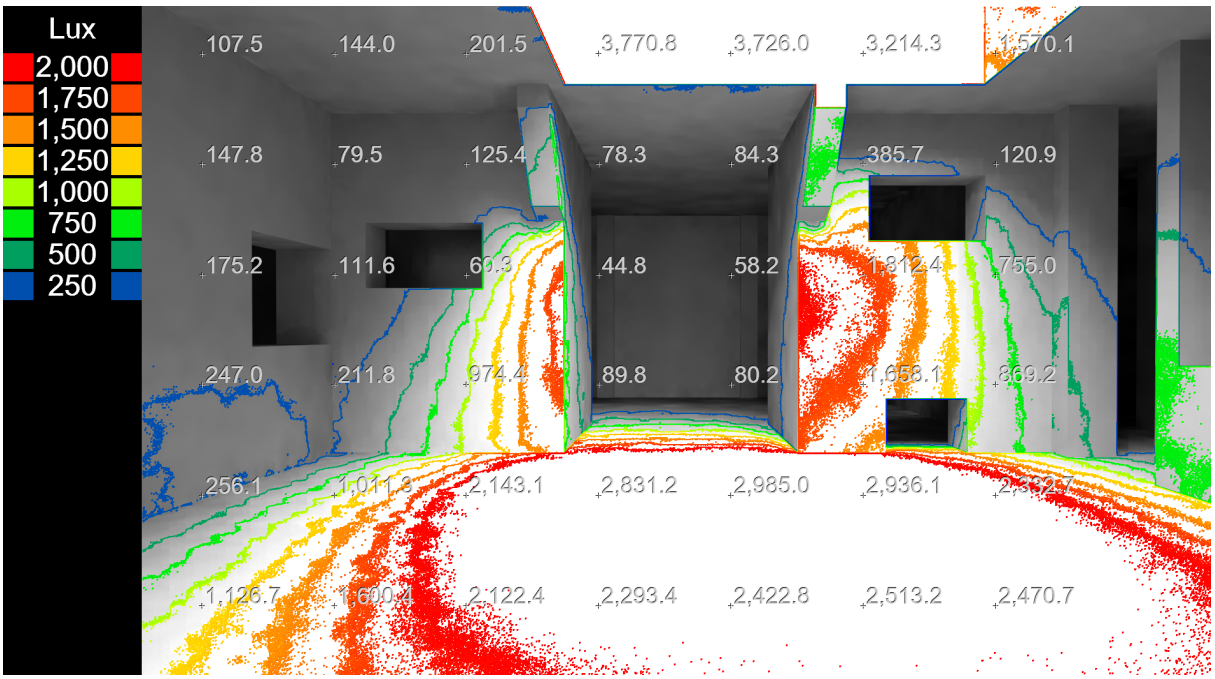


Figure 13. House 1—Courtyard (illuminance level at 21 June, 10 am).

This shows a distribution that concentrates daylight in peripheral, usable spaces. Inner rooms remain shaded. The morphological arrangement reconciles daylight needs with thermal control. Two distinct mechanisms produce this outcome. Spatial zoning allocates high illuminance to active courtyards and workspaces, where occupants need light for extended periods, while routing low illuminance to inner rooms used mainly for sleeping or storage. Morphological control—courtyard proportions, limited opening size, and wall depth—then regulates how much of that light, and the solar heat gain that travels with it, actually reaches the interior. Together these resolve the daylighting–thermal paradox: usable light where it is needed, minimal solar gain where it is not. The daylighting analysis of House-1 and House-2 shows that the central courtyard is the primary source of natural light. In both houses, workspaces such as living rooms, kitchens, corridors, staircases, and play areas receive adequate daylight. These spaces are mostly located near the courtyard or along circulation paths. Bedrooms, washrooms, and storage rooms receive lower daylight levels because they are placed at corner locations or along shared walls. This spatial arrangement reflects a deliberate climatic strategy. Spaces requiring longer daytime use are positioned where daylight is stronger. Private or sleeping areas remain more shaded. The result is a balanced distribution of light and thermal comfort. Lower daylight in corner rooms also reduces heat gain, since shared walls decrease direct solar exposure. This supports passive cooling objectives within dense traditional urban fabrics [21].

Daylight measurements indicate that most rooms record illuminance values below 250 lux, while courtyard and active zones reach approximately 300–2500 lux. These values align with the concept of Useful Daylight Illuminance (UDI), which evaluates the quality and usability of daylight rather than only its presence. UDI typically considers illuminance ranges around 100–300 lux as adequate for basic visual tasks, while 300–3000 lux is considered desirable for comfortable daytime use [22]. We classify our measured ranges against these UDI thresholds rather than compute a full annual UDI percentage: our illuminance data are single-time-point simulation snapshots (21 June, 10 am), not a continuous daylight-autonomy run across a representative sky-condition year, so we report where each zone falls on the UDI scale rather than the share of occupied hours within it. On that basis, courtyard and workspace readings (300–2500 lux) sit within or above the desirable UDI band, while inner rooms (<250 lux) sit at or below the minimum adequate threshold—consistent with the qualitative pattern the plan is organised around, though a full annual calculation would be needed to confirm it quantitatively. We list that as future work rather than assume it here. Supplementary Materials C provides the complete Velux Daylight Visualizer input parameters, sky model, and per-room lux outputs for both houses.

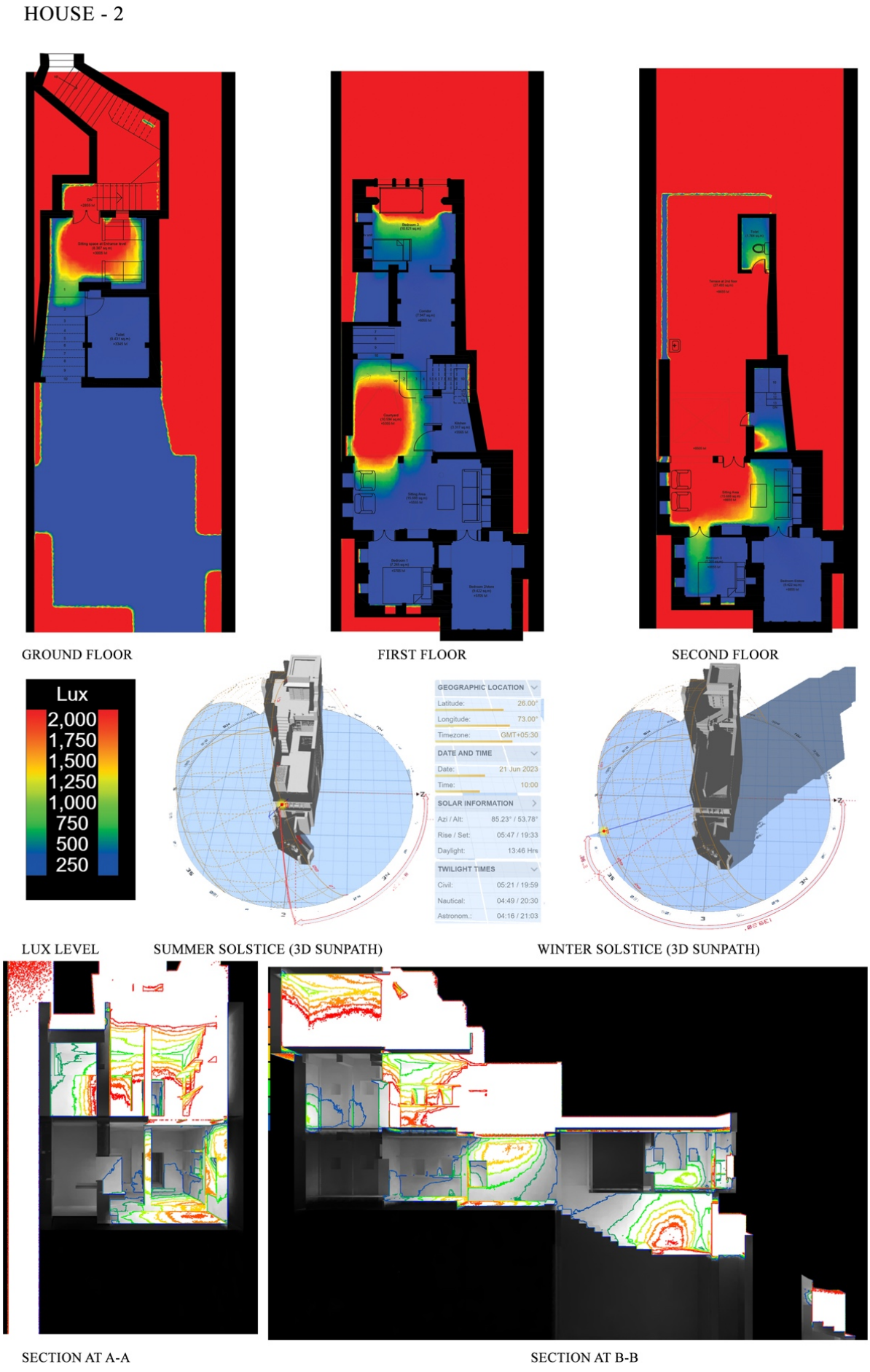


Figure 14. *Cont.*

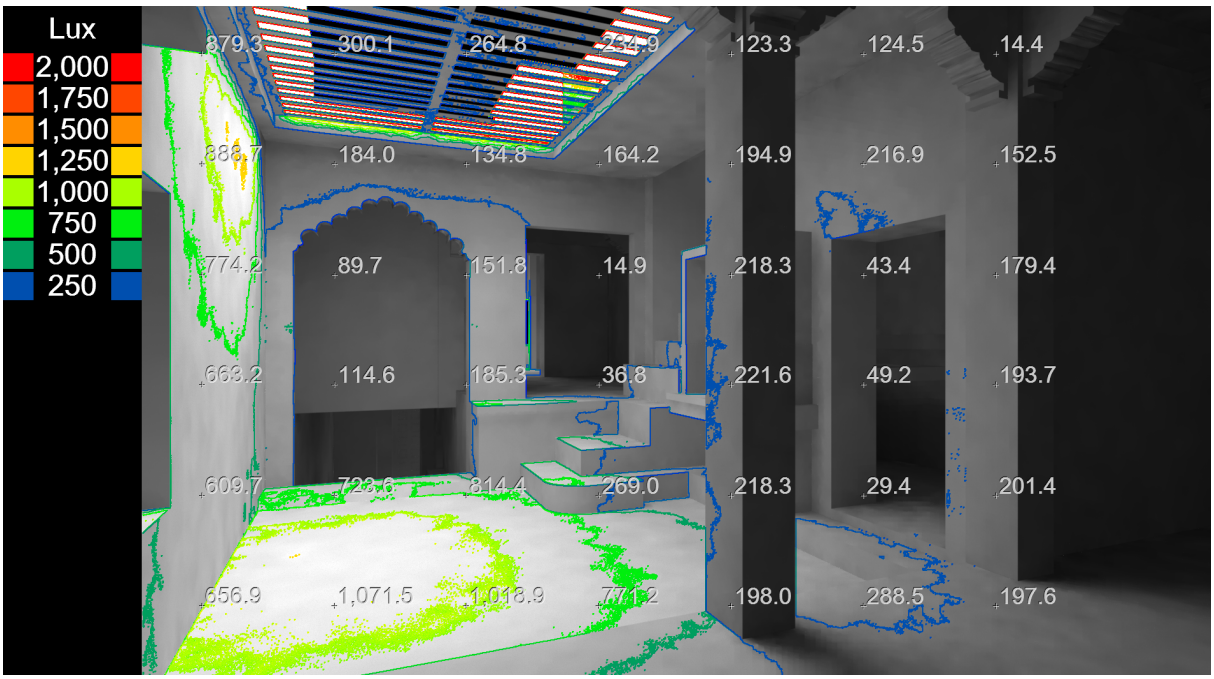


Figure 14. House 2—Courtyard (illuminance level at 21 June, 10 am).

4. Discussions & Conclusions: Scaling Building Performance to the City

4.1. Synthesis: Mechanism and Scaling

(1) At city scale, built-up intensity (NDBI) explains a large share of surface heat variance.
(2) At building scale, compact morphology reduces exposure and thermal mass creates damping.
(3) The combination means many well-formed buildings can alter district radiative conditions. Aggregate reduction in exposed surface lowers mean LST. Lower LST reduces night-time heat retention. This reduces urban heat accumulation.

Stated as a chain rather than three separate bullets, the argument runs: a form feature (compact plan, shared walls, courtyards) produces a physical mechanism (lower sky-view factor, mutual shading, and thermal mass with $U = 0.92\ W \cdot m^{-2} \cdot K^{-1}$ for stone walls), which we observe as a performance metric (indoor $\Delta T = 3.4$ °C, historic-core LST 0.63 °C cooler than the modern expansion), which we then argue—as a hypothesis rather than a demonstrated finding—aggregates into a systemic impact (lower district-mean LST and, potentially, reduced AC waste-heat rejection). Figure 15 sets out this chain explicitly; the first three links are supported by the measurements reported in Sections 2 and 3, and the fourth link is the conceptual claim examined in the upscaling discussion below.

We therefore treat morphology as a form of distributed thermal infrastructure at the building scale**:** a structural, passive mechanism that does not rely on mechanical energy. This contrasts with modern lightweight, glazed envelopes that rely on air conditioning, which raises electricity demand and, in many contexts, adds outdoor heat through waste-heat rejection—a feedback loop of higher ambient heat, higher cooling demand, and more waste heat. Traditional buildings interrupt this loop at the scale we measure it: the individual dwelling. Whether that interruption matters at district scale is the question the upscaling exercise below poses, not a conclusion we draw here.

We use a simple upscaling thought experiment. If a typical traditional dwelling provides $\Delta T = 3.4$ °C during peak hours, the local reduction in indoor cooling hours is material. If many dwellings in a block share this property, fewer occupants will use AC. Lower AC use reduces waste heat rejected to the street. Lower waste heat reduces local night-time ambient temperature. This feedback is complex and nonlinear. It depends on occupancy, AC penetration, and timing of heat release. We do not model the full system in this paper. We present the conceptual link and recommend system-level work that directly quantifies the feedback.

This chain rests on four assumptions we have not tested directly: (1) that the 3.4 °C interior moderation measured in two houses generalises across the historic core's wider building stock; (2) that occupants in AC-equipped buildings would actually reduce AC runtime in response to lower indoor peaks, rather than holding thermostat setpoints constant; (3) that waste heat rejected from AC condensers measurably raises street-level ambient temperature at block scale, given Jodhpur's built density and wind conditions; and (4) that this local waste-

heat effect feeds back into the same zones sampled for LST rather than dispersing elsewhere. Each assumption is supported elsewhere in the literature, but none is measured here; we present the argument as a conceptual link that motivates future system-level modelling, not as a demonstrated causal chain.

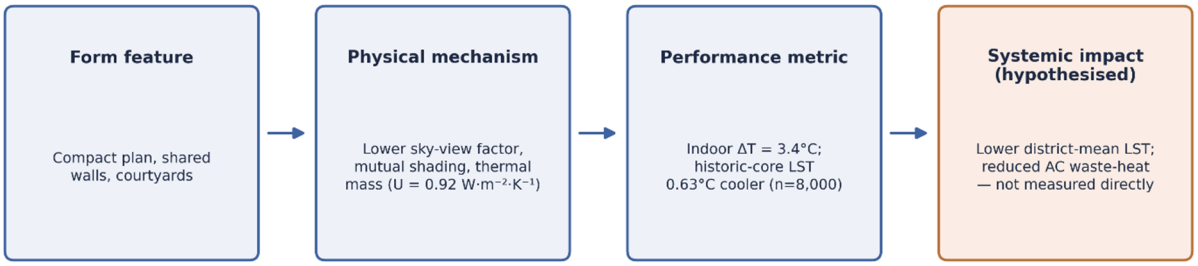


Figure 15. Morphology-as-infrastructure argument chain: form feature → physical mechanism → performance metric → systemic impact. The final link is hypothesised, not measured (see the upscaling discussion below).

Preserve and adapt traditional morphology as climate infrastructure. Pair morphology action with targeted greening. Amend national and local policies (ECBC, ICAP, Smart Cities, AMRUT, HRIDAY, municipal bylaws) to recognise and incentivise morphology-first measures.

We make this specific rather than aspirational. Table 1 sets out, instrument by instrument, what each currently measures, what we propose adding, and the finding from this study that motivates the addition.

Table 1. Policy gap analysis: current metrics vs. proposed morphology-linked additions.

Instrument	Current Metric/Focus	Proposed Morphology-Linked Addition	Finding Motivating It
ECBC	Envelope U-value and window-to-wall ratio limits, applied mainly to large commercial buildings	A compliance credit, or alternative compliance path, for designs demonstrating compact plans with courtyards and a minimum site-averaged Sky View Factor	Stone envelope U = 0.92 $W \cdot m^{-2} \cdot K^{-1}$ vs. brick U = 2.75 $W \cdot m^{-2} \cdot K^{-1}$; courtyard-linked indoor ΔT = 3.4 °C
ICAP	National cooling-demand-reduction target via non-technological measures (e.g., cool roofs); no built-form-specific metric	Recognise compact historic-fabric retention and courtyard retrofit as qualifying passive measures alongside cool roofs	NDBI is the dominant single driver of surface heat here (R^2 = 0.2776); compact fabric lowers exposed surface area per dwelling
Local planning bylaws (FAR, plot coverage, setback)	Regulate density and footprint; do not capture exposure or solar access	Add site-averaged Sky View Factor and façade-to-floor ratio as computable development-control metrics, usable as incentive triggers for bonus FAR	Transect peak-to-trough amplitude ≈ 8.09 °C tracks the boundary between low-SVF modern fabric and the compact historic core
Smart Cities Mission/AMRUT/ HRIDAY	Fund infrastructure upgrades and heritage conservation as separate line items from thermal performance	Fold morphology-based retrofit criteria into existing heritage and streetscape funding lines, rather than create a new scheme	Qualitative: avoids asking cities to create new budget lines for a measure this paper argues is already latent in the existing heritage stock

4.2. Key Conclusions

The present study provides evidence at two scales that traditional morphology functions as measurable thermal infrastructure in a hot-arid Indian city. Built-up intensity (NDBI) is the main contributor to surface heat at the urban scale. This explains more variance alone (R^2 = 0.28) than vegetation cover (R^2 = 0.01), and achieves R^2 = 0.55 when the two are combined. The historic core is, on average across 8000 sampled pixels, 0.63 °C cooler than the modern expansion. At the building scale, massive stone envelopes (U = 0.92 $W \cdot m^{-2} \cdot K^{-1}$) and courtyard-centred plans achieve a measured 3.4 °C indoor moderation relative to outdoor peaks. There is a daylight distribution of 300–2500 lux in active zones versus under 250 lux in inner rooms. This resolves the daylighting–thermal paradox through spatial zoning and morphological control, rather than mechanical means.

These findings also suggest treating traditional morphology as distributed thermal infrastructure. A passive, structural mechanism that reduces both surface and indoor heat without the electricity demand and waste heat feedback that mechanical cooling entails. The link between building-scale evidence and a city-scale cooling benefit is a stated hypothesis, rather than a demonstrated result. It relies on four assumptions that this study has not tested directly (Section 4.1). Closing that gap through morphology-resolved LST modelling is the clearest direction for future work. In the short term, the study translates directly into policy. The specific additions to ECBC, ICAP, local planning bylaws and the Smart Cities/AMRUT/HRIDAY. Evidences listed in Table 1 provide a route to credit this performance now, without waiting for that further evidence.

Supplementary Materials

The additional data and information can be downloaded at: https://media.sciltp.com/articles/others/2610121626515913/JHRR-26020127-SI.pdf.

Author Contributions

All authors contributed equally to the conceptualization, methodology, investigation, data curation, analysis, interpretation of results, and writing—original draft preparation and writing—review and editing. All authors have read and agreed to the published version of the manuscript and agree to be accountable for their respective contributions and for ensuring that questions related to the accuracy or integrity of the work are appropriately investigated, resolved, and documented. All authors have read and agreed to the published version of the manuscript.

Funding

This project was generously supported by the Swedish Postcode Foundation and ICCROM.

Institutional Review Board Statement

Not applicable. The study was limited to building temperature and humidity measurements, architectural documentation, observations of the built environment, and secondary data. It did not involve human or animal subjects.

Informed Consent Statement

Not applicable. The study did not involve human subjects.

Data Availability Statement

The data supporting the findings of this study are provided in the supplementary materials of this article. Additional information may be obtained from the corresponding author upon reasonable request.

Acknowledgments

Our interventions were conceived within the Net Zero framework of the FAR Programme of ICCROM and were generously supported by the Swedish Postcode Foundation.

Conflicts of Interest

The authors declare no conflict of interest.

Use of AI and AI-Assisted Technologies

Artificial intelligence tools (ChatGPT, OpenAI) were used in a limited capacity to support drafting, editing, and formatting of this paper. All content was reviewed and finalised by the authors.

References

1. Santamouris, M.; Cartalis, C.; Synnefa, A.; et al. On the impact of urban heat island and global warming on the power demand and electricity consumption of buildings—A review. *Energy Build.* **2015**, *98*, 119–124. https://doi.org/10.1016/j.enbuild.2014.09.052.
2. Ministry of Environment, Forest & Climate Change. *India Cooling Action Plan*; Ministry of Environment, Forest & Climate Change: New Delhi, India, 2019.

3. Mohajerani, A.; Bakaric, J.; Jeffrey-Bailey, T. The urban heat island effect, its causes, and mitigation, with reference to the thermal properties of asphalt concrete. *J. Environ. Manag.* **2017**, *197*, 522–538. https://doi.org/10.1016/j.jenvman.2017.03.095.
4. USGS. USGS Landsat 8 Level 2, Collection 2, Tier 1. 2013. Available online: https://developers.google.com/earth-engine/datasets/catalog/LANDSAT_LC08_C02_T1_L2 (accessed on 2 September 2026).
5. Malik, M.S.; Shukla, J.P.; Mishra, S. Relationship of LST, NDBI and NDVI using Landsat-8 data in Kandaihimmat Watershed, Hoshangabad, India. *Indian J. Geo-Mar. Sci.* **2019**, *48*, 25–31.
6. Roy, B.; Bari, E. Examining the relationship between land surface temperature and landscape features using spectral indices with Google Earth Engine. *Heliyon* **2022**, *8*, e10668. https://doi.org/10.1016/j.heliyon.2022.e10668.
7. Dirksen, M.; Ronda, R.J.; Theeuwes, N.E.; et al. Sky view factor calculations and its application in urban heat island studies. *Urban Clim.* **2019**, *30*, 100498. https://doi.org/10.1016/j.uclim.2019.100498.
8. Yin, S.; Liu, J.; Han, Z. Relationship between urban morphology and land surface temperature—A case study of Nanjing City. *PLoS ONE* **2022**, *17*, e0260205.
9. Verbeke, S.; Audenaert, A. Thermal inertia in buildings: A review of impacts across climate and building use. *Renew. Sustain. Energy Rev.* **2018**, *82*, 2300–2318. https://doi.org/10.1016/j.rser.2017.08.083.
10. Toris-Guitron, M.; Esparza-Lopez, C.J.; Luna-Leon, A.; et al. Evaluation of the thermal performance of traditional courtyard houses in a warm humid climate: Colima, Mexico. *npj Herit. Sci.* **2022**, *10*, 187.
11. Liu, Y.; Wang, W.; Li, Z.; et al. Daylighting Performance and Thermal Comfort Performance Analysis of West-Facing External Shading for School Office Buildings in Cold and Severe Cold Regions of China. *Sustainability* **2023**, *15*, 14458.
12. Guo, J.; Ren, H.; Zheng, Y.; et al. Evaluation of Land Surface Temperature Retrieval from Landsat 8/TIRS Images before and after Stray Light Correction Using the SURFRAD Dataset. *Remote Sens.* **2020**, *12*, 1023.
13. BEE. *Energy Conservation Building Code*; Bureau of Energy Efficiency, Ministry of Power: New Delhi, India, 2017.
14. ICCROM. Net Zero: Heritage for Climate Action. 2022. Available online: https://www.iccrom.org/projects/net-zero-heritage-climate-action (accessed on 2 September 2026).
15. Mardaljevic, J.; Andersen, M.; Roy, N.; et al. Daylighting Metrics: Is There a Relation Between Useful Daylight Illuminance and Daylight Glare Probability? In Proceedings of the First IBPSA-England Conference on Building Simulation and Optimization (BSO 2012), Loughborough, UK, 10–11 September 2012.
16. IMD. *Annual Climate Summary*; India Meteorological Department, Ministry of Earth Sciences: Pune, India, 2023.
17. Guha, S.; Govil, H. Evaluating the stability of the relationship between land surface temperature and land use/land cover indices: A case study in Hyderabad city, India. *Geol. Ecol. Landsc.* **2025**, *9*, 231–243. https://doi.org/10.1080/24749508.2023.2182083.
18. Brabant, C.; Dubreuil, V.; Dufour, S. Evaluation of spatial interpolation techniques for urban heat island monitoring in small and medium sized cities. *Front. Built Environ.* **2024**, *10*, 1455047. https://doi.org/10.3389/fbuil.2024.1455047.
19. Saha, B.; Lalrinmawia, V.; Singha, A.W. Traditional construction knowledge of the Blue City (Jodhpur): Paving way for a cooler future. Prevention Web. 2023. Available online: https://www.preventionweb.net/publication/traditional-construction-knowledge-blue-city-jodhpur-paving-way-cooler-future (accessed on 2 September 2026).
20. Kanji, R.; Madapala, J.; Sil, S. Culture for climate action in Jodhpur: reversing the trajectory from fragility to resilience. *J. Cult. Herit. Manag. Sustain. Dev.* **2024**, *14*, 787–804. https://doi.org/10.1108/JCHMSD-09-2022-0136.
21. Madapala, J.; Sil, S.; Kanji, R. Lessons from Jodhpur: Putting indigenous knowledge and place-based wisdom to practice. In *Encyclopedia of Disaster Risk Reduction*; Shaw, R., Ed.; Springer: Singapore, 2025; pp. 1–10. https://doi.org/10.1007/978-981-97-4547-0_233-1.
22. Kanji, R.; Madapala, J.; Sil, S. Co-building hyperlocal resilience: integrating the past with the present for a sustainable future—A framework for probable contextual replication from the old city of Jodhpur. *Humanit. Soc. Sci. Commun.* **2026**, *13*, 11. https://doi.org/10.1057/s41599-026-07811-x.